Raman spectroscopy of some natural hydrotalcites with sulphate and carbonate in the interlayer

Ray L. Frost•, Matt L. Weier, J.Theo Kloprogge
Inorganic Materials Research Program, School of Physical and Chemical Sciences, Queensland University of Technology, GPO Box 2434, Brisbane Queensland 4001, Australia.

Published as:
R.L. Frost, M.L. Weier, and J.T. Kloprogge, Raman spectroscopy of some natural hydrotalcites with sulphate and carbonate in the interlayer. Journal of Raman Spectroscopy, 2003. 34(10): p. 760-768.

Abstract

The structures of a series of nickel and magnesium based hydrotalcites have been explored using Raman microscopy. These natural hydrotalcites are based upon sulphate or carbonate being the counter anion in the interlayer. Variation in the position of the sulphate stretching vibrations occurs and is mineral dependent. Raman spectroscopy shows a reduction in the symmetry of both sulphate and carbonate, which leads to the conclusion that the anions are bonded to the brucite-like hydroxyl surface and to the water in the interlayer. Water bending modes are identified in both the Raman and infrared spectra at positions greater than 1630 cm^{-1}, indicating the water is strongly hydrogen bonded to both the interlayer anions and the hydrotalcite surface.

Key Words- hydrotalcite, brucite, Raman microscopy, carrboydite, hydrohonessite, takovite, mountkeithite.

INTRODUCTION

Hydrotalcites both natural and synthetic have been known for an extended period of time. [1-3] Early reports of natural hydrotalcites date back to 1944. [4] Hydrotalcites, or layered double hydroxides (LDH) are fundamentally known as anionic clays, and are less well-known and more diffuse in nature than cationic clays like smectites. [5] The structure of hydrotalcite can be derived from a brucite structure ($Mg(OH)_2$) in which e.g. Al^{3+} or Fe^{3+} (pyroaurite-sjögrenite) substitutes a part of the Mg^{2+}. [2,6-8] This substitution creates a positive layer charge on the hydroxide layers, which is compensated by interlayer anions or anionic complexes. In hydrotalcites a broad range of compositions are possible of the type $[M^{2+}_{1-x}M^{3+}_{x}(OH)_2]_{x/n}.yH_2O$, where M^{2+} and M^{3+} are the di- and trivalent cations in the octahedral positions within the hydroxide layers with x normally between 0.17 and 0.33. A^{n-} is an exchangeable interlayer anion. [9]

• Author to whom correspondence should be addressed (r.frost@qut.edu.au)

There exists in nature a significant number of hydrotalcites which are formed as deposits from ground water containing Ni^{2+} and Fe^{3+}. [10] These are based upon the dissolution of Ni-Fe sulphides during weathering. Among these naturally occurring hydrotalcites are carrboydite and hydrohonessite [11,12]. These two hydrotalcites are based upon the incorporation of sulphate into the interlayer with expansions of 10.34 to 10.8 Å. Normally the hydrotalcite structure based upon takovite (Ni,Al) and hydrotalcite (Mg,Al) has basal spacings of ~8.0 Å where the interlayer anion is carbonate. If the carbonate is replaced by sulphate then the mineral carrboydite is obtained. Similarly reevesite is the (Ni,Fe) hydrotalcite with carbonate as the interlayer anion, which when replaced by sulphate the minerals honessite and hydrohonessite are obtained. Table 1 shows the names of the minerals with different interlayer anions, their d(001) spacing along the C-axis. [10]

Insert Table 1 here

Interest in the study of hydrotalcites results from their potential use as catalysts. [13-17] The reason rests with the ability to make mixed metal oxides at the atomic level, rather than at a particle level. Such mixed metal oxides are formed through the thermal decomposition of the hydrotalcite. [18,19] Hydrotalcites may also be used as a components in new nano-materials such as nano-composites. [20] There are many other uses of hydrotalcites. Hydrotalcites are important in the removal of environmental hazards in acid mine drainage. [21,22] Hydrotalcite formation offers a mechanism for the disposal of radioactive wastes. [23] Hydrotalcite formation may also serve as a means of heavy metal removal from contaminated waters. [24]

The characterisation of these types of minerals by infrared spectroscopy has been well documented. [13] More recently, infrared emission spectroscopy has been used to study the thermal behaviour of hydrotalcites. One of the disadvantages of infrared spectroscopy in the study of hydrotalcites is that the water in the hydrotalcite is such an intense absorber, and may mask the absorbance of the MOH units. One of the advantages of Raman spectroscopy is that water is a very poor scatterer. Thus the hydroxyl stretching of the MOH units may be readily observed. However few reports of the Raman spectroscopy of these hydrotalcite minerals either natural or synthetic have been forthcoming. [8,9,11] The application of Raman spectroscopy to the study of synthetic Co/Al and Ni/Al hydrotalcites has shown the reduced symmetry of the carbonate in the interlayer. [25] The effect of cation size on hydrotalcite stability has been studied using vibrational spectroscopic techniques. [26] in-situ infrared and Raman spectroscopy has been sued to determine the thermal stability of as-synthesised Co/Al and Ni/Al hydrotalcites. [25,26] In this paper we report the changes in the structure of a set of natural hydrotalcites using Raman microscopy.

EXPERIMENTAL

The Minerals

Hydrotalcites were obtained from a number of Australian deposits.
Honessite (Reg. No. 25175) came from Otter Shoot, Western Australia.
Hydrohonessite (Reg. No, 26550) originated from Kambalda, Western Australia.
Reevesite (Reg. No. 17316) was sourced from Nullagine, Western Australia.
Carrboydite (Reg. No. G26549) came from Widgemoulth, Western Australia.
The carrboydite and takovite were supplied by CSIRO.

The minerals were checked for composition by an electron probe.

Raman microprobe spectroscopy

The crystals of hydrotalcite minerals were placed and orientated on a polished metal surface on the stage of an Olympus BHSM microscope, which is equipped with 10x and 50x objectives. The microscope is part of a Renishaw 1000 Raman microscope system, which also includes a monochromator, a filter system and a Charge Coupled Device (CCD). Raman spectra were excited by a Spectra-Physics model 127 He-Ne laser (633 nm) at a resolution of 2 cm^{-1} in the range between 100 and 4000 cm^{-1}. Repeated acquisition, using the highest magnification, was accumulated to improve the signal to noise ratio in the spectra. Spectra were calibrated using the 520.5 cm^{-1} line of a silicon wafer. Powers of less than 1 mW at the sample were used to avoid laser induced degradation of the sample. [27-29] Slight defocusing of the laser beam also assists in the preservation of the sample.

Spectroscopic manipulation such as baseline adjustment, smoothing and normalisation were performed using the Spectracalc software package GRAMS (Galactic Industries Corporation, NH, USA). Band component analysis was undertaken using the Jandel 'Peakfit' software package, which enabled the type of fitting function to be selected and allows specific parameters to be fixed or varied accordingly. Band fitting was done using a Gauss-Lorentz cross-product function with the minimum number of component bands used for the fitting process. The Gauss-Lorentz ratio was maintained at values greater than 0.7 and fitting was undertaken until reproducible results were obtained with squared correlations of r^2 greater than 0.995.

RESULTS AND DISCUSSION

The hydrotalcites used in this study are natural and have been formed by deposition from solution. The solutions are formed from the oxidised zones of pyrite ore bodies. These are based upon the dissolution of Ni-Fe sulphides during weathering. The hydrotalcites are formed at the appropriate pH and solution chemistry. This means the interlayer anion is whatever anion is available in solution during precipitation. More often than not the anions are sulphate or carbonate; and more likely there is a mixture of the two anions in the hydrotalcite interlayer. Thus the hydrotalcites based upon Ni as the divalent ion is $Ni_6Al_2(OH)_{16}(CO_3).4H_2O$ and $Ni_6Fe_2(OH)_{16}(CO_3).4H_2O$ depending on which is the trivalent cation. These are the two minerals takovite and reevesite. If sulphate is the predominant anion the two minerals are carrboydite and hydrohonessite (Table 1). If Mg replaces the Ni in these two minerals then the minerals motukoreaite and mountkeithite are obtained. Thus Raman spectroscopy of the hydrotalcites will identify bands associated with the hydroxyl stretching vibrations of the MOH units, the water, and the interlayer anions. Thus the hydroxyl stretching of the MOH units may be readily observed. However few reports of the Raman spectroscopy of these hydrotalcite minerals either natural or synthetic have been forthcoming.

Hydroxyl Stretching Region

In hydrotalcites water can be present in various forms. In general one can recognise water in the interlayer between the hydroxide layers, which may or may not form bridging-type bonds with the exchangeable anions and water adsorbed on the outer surface plus finally free water in between the particles. Water bending modes can be recognised in mainly the infrared spectra between roughly 1500 and 1700 cm^{-1} accompanied by OH-stretching vibrations in the 3000-4000 cm^{-1} region. In the Raman spectra these bands are generally very weak or even absent, especially the bending vibrations. Depending on the strength with which the water molecule is hydrogen-bonded to other molecules a shift can be observed in the spectra towards higher wavenumber in the bending region in contrast to the stretching region where a shift to lower wavenumber is observed. Normally minerals containing physically adsorbed water give strong infrared bands around 3450 cm^{-1} and 1630 cm^{-1}. Generally speaking monomeric, non-hydrogen bonded water such as occurs in the vapour phase gives bands around 3755 and 1595 cm^{-1}, while in the liquid phase these bands shift to 3455 and 1645 cm^{-1} and in ice to 3255 and 1655 cm^{-1}.

When water is bound to the surface of a mineral the strength of the hydrogen bond will determine where the OH-bending and stretching vibration will be observed. For water adsorbed on clay minerals the OH-stretching modes of weak hydrogen bonds occur in the region between 3580 and 3500 cm^{-1} while strong hydrogen bonds are observed below 3420 cm^{-1}. When water is coordinated to cations in cationic clay minerals the stretching vibration occurs around 3220 cm^{-1} corresponding to an ice-like structure. In both cationic clay minerals and hydrotalcites a strong overlap exists in the OH-stretching region between the M-OH bands of the hydroxide layers and the OH-bands of water. Therefore, for the study of water in and on hydrotalcites the OH-bending region of the infrared spectrum is much more informative. For all hydrotalcites this band is observed in the range between roughly 1580 and 1655 cm^{-1}. No clear effect can be seen due to variation in either the divalent or the trivalent cations present in the hydroxide layers. The interlayer anion however does have a significant effect on the position of the OH-bending mode of the interlayer water. Similar values are observed for carbonate and sulphate anions, but a significant shift towards lower wavenumbers by about 20 cm^{-1} is observed for hydroxyl and nitrate interlayer anions.

The Raman spectrum of the high wavenumber region of the series of hydrotalcites is shown in Figure 1. The results of the Raman spectral analyses are reported in Table 1. The Raman spectrum of the hydroxyl stretching region of carrboydite shows a sharp band at 3614 cm^{-1} and a broad continuum centred upon 3445 cm^{-1}. The bandwidth of the 3614 cm^{-1} band is 69.7 cm^{-1}. The first band may be assigned to AlOH stretching vibrations as bands in similar positions are observed for the kaolinite clay minerals. The broad continuum must be associated with NiOH and water stretching vibrations. In contrast the spectra of the hydroxyl stretching region of hydrohonessite, mountkeithite and reevesite show sharp bands. These bands are attributed to MOH stretching vibrations. The bands in the hydroxyl stretching region of hydrohonessite are found at 3493 and 3445 cm^{-1} with bandwidths of 28.7 and 56.8 cm^{-1}. The Raman spectrum of mountkeithite displays bands at 2698, 3688 and 3654 cm^{-1}. The Raman spectrum of reevesite in the hydroxyl stretching region strongly resembles that of hydrohonessite. This is not unexpected as the two minerals only differ by having different anions in the interlayer.

Sulphate vibrations

The free sulphate anion SO_4^{2-} has a site symmetry of T_d corresponding to a space group of O_h^7 with the $\nu_3(F)$ and $\nu_4(F)$ modes both Raman and infrared active, while the $\nu_1(A_1)$ and $\nu_2(E)$ modes are only Raman active with ν_1 around 981, ν_2 around 451, ν_3 around 1104 and ν_4 around 613 cm^{-1}. Good examples of hydrotalcites with sulphate in the interlayer are honessite, hydrohonessite and carrboydite. The Raman spectrum of the SO_4 and CO_3 stretching vibrations are shown in Figure 2 and the results reported in Table 1. Carrboydite is characterised by an intense band centred at 981 cm^{-1} and is assigned to the SO_4 symmetric stretching vibration. A very broad band for carrboydite is observed at around 1125 cm^{-1} and this must be the observation of the Raman bands of the SO_4 antisymmetric stretching vibrations. The infrared spectrum of carrboydite shows three bands at 1088, 1021 and 978 cm^{-1}. The first two bands are due to the intense SO_4 antisymmetric stretching vibrations and the last band is the weak infrared SO_4 symmetric stretching vibration. No carbonate bands at around 1060 cm^{-1} was observed in the Raman spectrum; thus indicating the carrboydite was a pure sulphate mineral with no carbonate exchange. The 981 cm^{-1} band is broad with bandwidth of 28.7 cm^{-1}. In contrast, the Raman spectrum of both hydrohonessite and reevesite show sharp bands at 1008 cm^{-1} with bandwidths of 5.5 cm^{-1}. Hydrohonessite Raman spectrum shows two bands at 1135 and 1115 cm^{-1} with bandwidths of 8.2 and 26.1 cm^{-1}. The reevesite Raman spectrum displays two bands at 1135 and 1118 cm^{-1} with bandwidths of 10.4 and 16.7 cm^{-1}. The infrared spectrum of hydrohonessite shows two intense bands at 1088 and 1021 cm^{-1}. A very weak band is observed at 978 cm^{-1}. In comparison the bandwidths of the infrared peaks are very broad. The Raman spectrum of mountkeithite displays two bands at 1129 and 1109 cm^{-1}, assigned to the SO_4 antisymmetric stretching vibrations.

Bish and Livingstone observed for honessite the sulphate ν_1, ν_2, ν_3 and ν_4 modes at 980, 500, 1140 and 650 cm^{-1}, respectively. [11] The ν_3 mode is clearly split but no separate band positions were given. The infrared spectrum of synthetic hydrohonessite was very similar to that of the naturally occurring honessite. [11]Although the split of the ν_3 mode is only visible as a weak shoulder on the low wavenumber side of the comparatively broad band in contrast to the (hydro)honessite, where the weaker of the two bands is observed as a separate band or shoulder at the higher wavenumber side. The fact that these authors found all four modes to be infrared active indicates that the symmetry of the sulphate anion has been lowered from T_d for the free anion to C_3 or C_{3v}, which would result in activation of the two infrared inactive modes plus splitting of the ν_3 mode. Dutta and Puri observed bands associated with the sulphate anion in Li/Al-hydrotalcite in the Raman spectrum around 457, 467, 620 (all three weak), 986 and 1116 cm^{-1} (broad). The splitting of ν_2 and the broadening of the antisymmetric stretching mode ν_3 indicate a significant symmetry lowering. [30] Dutta and Puri suggested D_2 which is however not compatible with the infrared data where all four bands have been observed. [30] For similar reasons C_3 site symmetry as suggested by Bish is not compatible with the Raman data. Therefore, based on combined observations in both the infrared and Raman spectra the conclusion has to be that the site symmetry is most probably C_{2v} or C_s with ν_1 A_1 infrared and Raman active, ν_2 A_1 infrared and Raman active, ν_2 A_2 only Raman active, and ν_3 and ν_4 $A_1 + B_1 + B_2$ all infrared and Raman active.

The Raman spectra of the low wavenumber region are shown in Figure 3. The Raman spectrum of hydrohonessite displays bands at 671, 619 and 579 cm^{-1}. These bands are attributed to the SO_4 ν_4 bending modes. The first two bands have halfwidths of 6.8 and 12.2 cm^{-1}. The last band is broad with a bandwidth of 46.8 cm^{-1}. Two additional bands are observed at 493 and 414 cm^{-1} and are attributed to the ν_2 bending modes. The bandwidths are 10.1 and 8.2 cm^{-1}. The Raman bands for reevesite show similarity in band position; however there are significant differences in intensity. Bands are observed at 670, 619 and 586 cm^{-1} for the ν_4 vibrations with bandwidths of 6.3, 12.7 and 53.2 cm^{-1}. The ν_2 modes for reevesite are observed at 493 and 414 cm^{-1} with bandwidths of 10.3 and 8.1 cm^{-1}. The bands for carrboydite may be compared. In this example, the Raman spectrum shows quite broad overlapping bands in both the ν_2 and ν_4 regions. For carrboydite, the ν_4 bands are observed at 631, 613, 563 and 552 cm^{-1} with bandwidths of 28.9, 30.2, 46.5 and 15.5 cm^{-1}. The ν_2 bands are observed at 499, 457 and 403 cm^{-1}.

Carbonate vibrations

Only a very limited number of Raman studies have been reported so far on the interlayer carbonate anion in hydrotalcites. Takovite is an example of a naturally occurring hydrotalcite with carbonate as the interlayer anion. When the carbonate species is present as a free ion not involved in any bonding it will exhibit a space group of D_{3h}. In the Raman spectrum one will observe $\nu_1(A'1)$, $\nu_3(E')$ and $\nu_4(E')$. As a result three bands, the bending non-planar mode $\nu_2(A''2)$, the anti-symmetrical stretching mode $\nu_3(E')$ and the bending angular mode $\nu_4(E')$, will be observed in the infrared spectrum around 880, 1415 and 680 cm^{-1}, while the symmetric stretching mode $\nu_1(A'1)$ is infrared inactive. However, changes can be expected when the carbonate ion is intercalated in the hydrotalcite structure as it will be affected by interactions with interlayer water molecules and/or OH-groups from the hydrotalcite layers. In comparison with free CO_3^{2-} a shift towards lower wavenumbers is generally observed. Interaction between interlayer water molecules and the carbonate ion is reflected by the presence in the OH-stretching region of the infrared spectrum around 3000-3100 cm^{-1}

The shift towards lower wavenumbers indicates a loss of freedom compared to free CO_3^{2-} and as a consequence a lowering of the carbonate symmetry from D_{3h} to probably C_{2s} or C_v. The Raman spectrum of takovite displays intense Raman band at 1060 cm^{-1} with a low intensity band at 1042 cm^{-1}. The position of this band may be compared with the values for witherite and cerrusite where positions of 1063 and 1053 cm^{-1} are observed. No bands are also observed at around 1350 cm^{-1} which would be attributed to the antisymmetric stretching vibrations. The infrared spectrum of takovite shows two bands at 1351 and 1417 cm^{-1}. These frequencies may be compared with those of aragonite where bands are observed at 1466 and 1464 cm^{-1}; strontiantite at 1450 and 1400 cm^{-1}. As a result of this symmetry lowering the infrared inactive ν_1 mode will be activated. Indeed, a weak band has been observed around 1050-1060 cm^{-1}. In addition the ν_3 mode shows a small splitting in the order of 30-60 cm^{-1}. Some papers have only reported the activated ν_1 in combination with a single ν_3 band. In these cases the ν_3 band seems to be broadened due to an overlap of the two split modes ν_3 and ν_{3a}.

For takovite a band is observed at 687 cm^{-1} and is attributed to the ν_4 mode. An intense band is observed at 558 cm^{-1} and is attributed to the ν_2 mode. Two low intensity bands are observed at 533 and 492 cm^{-1}. However, for the ν_4 mode Kloprogge and Frost reported a minor sharp band at 694 cm^{-1}, which indicates a similar sized shift but in opposite direction. A reasonable explanation for this band was given by Kagunya et al., who showed the presence of a band at 698 and 695 cm^{-1} in the Raman spectra of Mg/Al-hydrotalcites with OH^- and CO_3^{2-} as interlayer anion, respectively and assigned this vibration as the $E_{g(T)}$ mode. [31] This band will then fully overlap the much weaker carbonate ν_4 mode. Detailed examination of the 694 cm^{-1} band indicates a rather sudden broadening supporting an overlap between these two bands. Similarly, Kagunya et al. gave an alternative assignment for the 1060 cm^{-1} band as the $E_{g(R)}$ (OH) mode, which they observed in both the carbonate and the hydroxyl interlayered LDHs. [31]

Water HOH deformation vibrations

Water is a poor Raman scatterer and the Raman spectra of water vibrational modes are difficult to obtain. Nevertheless the Raman spectra of selected hydrotalcites are shown in Figure 4. Often significant information can be obtained through the study of the water bending modes centred on 1620 cm^{-1}. The Raman spectrum of this region for carrboydite shows a band at 1625 cm^{-1}, for reevesite at 1635 cm^{-1} and for hydrohonessite at 1638 cm^{-1}. The water hydroxyl bending region is complex with more than one band being observed. For the study of the water bending modes it is far better to use infrared spectroscopy.

For carrboydite two infrared bands are observed at 1661 and 1620 cm^{-1}. A very low intensity band is also observed at 1485 cm^{-1}. This latter band may be assigned to the CO_3 antisymmetric stretching vibrations. The significance of two water bending modes rests with water being involved in the hydrotalcite structure with two different hydrogen bond strengths. The band at 1661 cm^{-1} results form water being strongly hydrogen bonded. Two possibilities exist (a) hydrogen bonding to the OH units of the hydroxyl surface and (b) hydrogen bonding to the sulphate. The second type of water is more relatively weakly hydrogen bonded and it is suggested that this type of water molecule is hydrogen bonded to the sulphate anion in the interlayer structure. It is apparent that the water is in a structured environment in the hydrotalcite interlayer. For hydrohonessite, two bands are observed at 1656 and 1595 cm^{-1}. The relative intensities of the two bands are 2:1. Most of the water molecules are strongly hydrogen bonded in the hydrohonessite structure. For motukoreaite, the water bending mode is observed at 1645 cm^{-1}. The band overlaps with carbonate antisymmetric vibrations observed at 1422 and 1472 cm^{-1}. The observation of water bending modes at positions higher than 1630 cm^{-1} supports the concept of 'structured' water in the hydrotalcite structure. The carbonate is present as an isomorphic substitute for sulphate in the motukoreaite structure. In comparison the water bending mode for takovite is a weak shoulder on the carbonate antisymmetric stretching vibration profile. The band is observed at 1632 cm^{-1}. Thus the position of the water bending mode is a measure of the hydrogen bonding strength in the hydrotalcite structure. The order of hydrogen bonding is carrboydite, hydrohonessite, motukoreaite, takovite. What this spectroscopic evidence shows is that the hydrogen bonding of water in the interlayer is not the same for each hydrotalcite. Such a concept can be extrapolated to a measure of the stability of the hydrotalcite.

CONCLUSIONS

Hydrotalcites have a unique structure in that the mineral acts like an anionic clay with a 'giant' cation whose charge is counterbalanced by multiple anions in the interlayer. Hydrotalcites are normally not easy to measure in terms of Raman spectroscopy because of their small particle size together with their disordered nature. The Raman spectroscopy of the natural hydrotalcites has the benefit that the crystallization has taken place over eons of time and consequently the particles are sufficiently large to be observed using the Raman microscopic technique. Nevertheless such a mineral has been deposited from a solution from an oxidised zone of base metal ore bodies and as such the mineral has to be measured against the background of some rock matrix. The other difficulty with the measurement of hydrotalcites is that those based upon nickel or nickel with some copper can be highly coloured and are likely to be susceptible to laser degradation. This can be readily observed under the optical microscope. Such laser induced decomposition may result in dehydration, dehydroxylation and even de-carbonation of the hydrotalcite. Such phenomena can be observed by changes in the Raman spectrum as the data is collected. The use of low power densities and slight defocusing of the laser assists in the collection of spectra without damage to precious (and sometimes rare) minerals.

In this work, the Raman spectra of the interlayer anions of carbonate and sulphate have been collected. The splitting of the ν_3, ν_4 and ν_2 modes indicates symmetry lowering of the carbonate and sulphate anions. The symmetry lowering must be taken into count through the bonding of the sulphate and carbonate anions to both water and the brucite-like hydroxyl surface. Water plays an essential role in the hydrotalcite structure as may be evidenced by the position of the water bending modes. The water is strongly hydrogen bonded to both the anions and the hydroxyl surface. Raman spectroscopy has the advantage of water being a very poor scatterer and hence is difficult to observe compared with IR spectroscopy. Thus the cation OH stretching vibrations are more readily observed with Raman spectroscopy.

Acknowledgments

The financial and infra-structure support of the Queensland University of Technology Inorganic Materials Research Program is gratefully acknowledged. The Australian Research Council (ARC) is thanked for funding. Prof. Allan Pring of the South Australian Museum is thanked for the loan of some of the hydrotalcite minerals. Dr Ernie Nickel is thanked for the supply of several of the hydrotalcites.

References

1. Allmann, R. *Acta Crystallographica, Section B: Structural Crystallography and Crystal Chemistry* 1968**; 24**: 972.
2. Ingram, L, Taylor, HFW. *Mineralogical Magazine and Journal of the Mineralogical Society (1876-1968)* 1967**; 36**: 465.
3. Taylor, HFW. *Mineralogical Magazine* 1973**; 39**: 377.
4. Caillere, S. *Compt. rend.* 1944**; 219**: 256.
5. Rives, V, Editor *Layered Double Hydroxides: Present and Future*, 2001.
6. Brown, G, Van Oosterwyck-Gastuche, MC. *Clay Minerals* 1967**; 7**: 193.

7. Taylor, HFW. *Mineralogical Magazine and Journal of the Mineralogical Society (1876-1968)* 1969**; 37**: 338.
8. Taylor, RM. *Clay Minerals* 1982**; 17**: 369.
9. Kloprogge, JT, Wharton, D, Hickey, L, Frost, RL. *American Mineralogist* 2002**; 87**: 623.
10. Nickel, EH, Wildman, JE. *Mineralogical Magazine* 1981**; 44**: 333.
11. Bish, DL, Livingstone, A. *Mineralogical Magazine* 1981**; 44**: 339.
12. Nickel, EH, Clarke, RM. *American Mineralogist* 1976**; 61**: 366.
13. Theo Kloprogge, J, Frost, RL. *Applied Catalysis, A: General* 1999**; 184**: 61.
14. Alejandre, A, Medina, F, Rodriguez, X, Salagre, P, Cesteros, Y, Sueiras, JE. *Appl. Catal., B* 2001**; 30**: 195.
15. Das, J, Parida, K. *React. Kinet. Catal. Lett.* 2000**; 69**: 223.
16. Patel, SH, Xanthos, M, Grenci, J, Klepak, PB. *J. Vinyl Addit. Technol.* 1995**; 1**: 201.
17. Rives, V, Labajos, FM, Trujillano, R, Romeo, E, Royo, C, Monzon, A. *Appl. Clay Sci.* 1998**; 13**: 363.
18. Rey, F, Fornes, V, Rojo, JM. *J. Chem. Soc., Faraday Trans.* 1992**; 88**: 2233.
19. Valcheva-Traykova, M, Davidova, N, Weiss, A. *J. Mater. Sci.* 1993**; 28**: 2157.
20. Oriakhi, CO, Farr, IV, Lerner, MM. *Clays Clay Miner.* 1997**; 45**: 194.
21. Lichti, G, Mulcahy, J. *Chemistry in Australia* 1998**; 65**: 10.
22. Seida, Y, Nakano, Y. *Journal of Chemical Engineering of Japan* 2001**; 34**: 906.
23. Roh, Y, Lee, SY, Elless, MP, Foss, JE. *Clays and Clay Minerals* 2000**; 48**: 266.
24. Seida, Y, Nakano, Y, Nakamura, Y. *Water Research* 2001**; 35**: 2341.
25. Perez-Ramirez, J, Mul, G, Moulijn, JA. *Vib. Spectrosc.* 2001**; 27**: 75.
26. Perez-Ramirez, J, Mul, G, Kapteijn, F, Moulijn, JA. *J. Mater. Chem.* 2001**; 11**: 2529.
27. Martens, W, Frost, RL, Kloprogge, JT, Williams, PA. *Journal of Raman Spectroscopy* 2003**; 34**: 145.
28. Frost, RL, Martens, W, Kloprogge, JT, Williams, PA. *Journal of Raman Spectroscopy* 2002**; 33**: 801.
29. Frost, RL, Martens, WN, Williams, PA. *Journal of Raman Spectroscopy* 2002**; 33**: 475.
30. Dutta, PK, Puri, M. *Journal of Physical Chemistry* 1989**; 93**: 376.
31. Kagunya, W, Baddour-Hadjean, R, Kooli, F, Jones, W. *Chemical Physics* 1998**; 236**: 225.

Anion	Divalent cation	Trivalent cation	Mineral
Carbonate (~8 Å)	Ni	Al	takovite
	Mg	Al	hydrotalcite
	Mg	Fe	pyroaurite
	Ni	Fe	reevesite
Sulphate (~9 Å)	Ni	Fe	honessite
Sulphate (~10-11 Å)	Mg	Al	motukoreaite
	Ni	Al	carrboydite
	Ni	Fe	hydrohonessite
	Mg	Fe	mountkeithite

Table 1 Table of the natural hydrotalcite minerals with sulphate or carbonate in the interlayer

Table 2 Results of the Raman spectral analysis of selected hydrotalcites

Carrboydite	Centre				3614		3445													1125				
	FWHM				69.7		288.5													88.8				
	Rel. Area				0.024		0.230													0.065				
Hydrohonessite	Centre					3493		3405											1135		1115			1008
	FWHM					28.7		56.8											8.2		26.1			5.6
	Rel. Area					0.142		0.075											0.109		0.034			0.379
Mountkeithite	Centre	3698	3688	3654							2240	1937	1679	1613		1525	1439	1273			1122	1109		
	FWHM	8.9	13.6	32.6							1.4	181.4	94.5	99.2		122.4	61.9	46.2			40.3	40.3		
	Rel. Area	0.024	0.020	0.009							0.002	0.035	0.127	0.139		0.179	0.087	0.124			0.093	0.093		
Reevesite	Centre					3492		3406											1135		1118			1008
	FWHM					29.3		66.0											10.4		16.7			5.5
	Rel. Area					0.105		0.062											0.085		0.028			0.429
Takovite	Centre						3461		2855	2615					1543							1060	1042	
	FWHM						169.6		230.0	165.8					1089.5							11.6	36.9	
	Rel. Area						0.094		0.045	0.029					0.245							0.080	0.091	

Carrboydite	Centre	981	981				631		613		563	552		499	457		403			318
	FWHM	28.7	15.3				28.9		30.2		46.5	15.5		43.4	43.0		28.9			27.1
	Rel. Area	0.150	0.197				0.028		0.018		0.083	0.005		0.066	0.067		0.010			0.010
Hydrohonessite	Centre					671		619		579				493		414				318
	FWHM					6.8		12.2		46.8				10.1		8.2				24.0
	Rel. Area					0.035		0.031		0.021				0.016		0.066				0.005
Mountkeithite	Centre			920	691			621					528		468		390	348		
	FWHM			101.8	11.0			11.2					16.5		11.6		9.1	5.8		
	Rel. Area			0.024	0.049			0.005					0.011		0.002		0.040	0.005		
Reevesite	Centre					670		619		586				493		414				314
	FWHM					6.3		12.7		53.2				10.3		8.1				16.1
	Rel. Area					0.013		0.042		0.024				0.084		0.046				0.007
Takovite	Centre	992			687						558		533	492			403		324	
	FWHM	69.2			43.2						15.3		10.0	20.5			16.2		25.0	
	Rel. Area	0.071			0.027						0.162		0.005	0.034			0.008		0.004	

Carrboydite	Centre	248	227		205		
	FWHM	13.1	29.8		17.2		
	Rel. Area	0.002	0.006		0.003		
Hydrohonessite	Centre			209		182	164
	FWHM			25.2		10.6	7.4
	Rel. Area			0.023		0.025	0.002
Mountkeithite	Centre		233		202		
	FWHM		10.0		7.2		
	Rel. Area		0.025		0.001		
Reevesite	Centre			212		181	
	FWHM			23.5		10.2	
	Rel. Area			0.015		0.021	
Takovite	Centre	253	225	218			
	FWHM	10.3	4.0	3.9			
	Rel. Area	0.003	0.003	0.003			

List of Tables

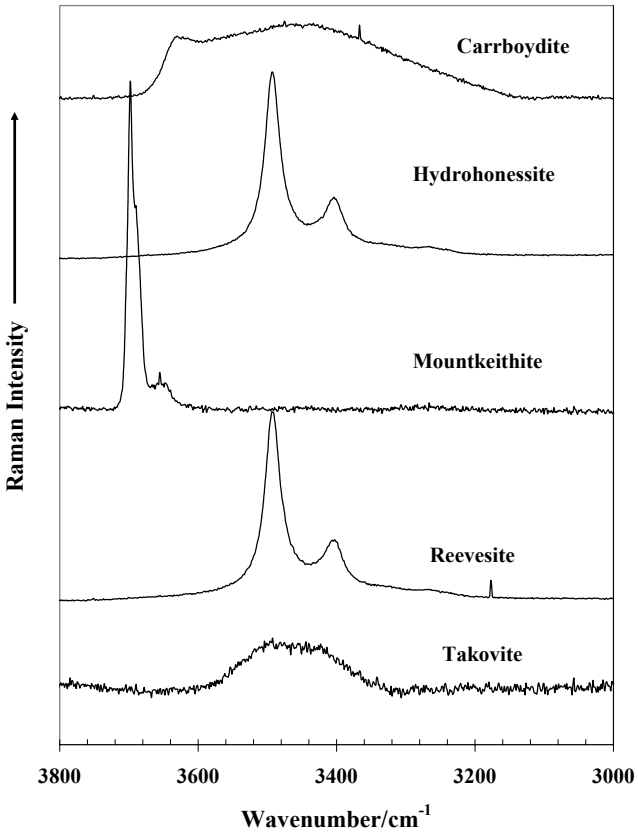

Figure 1 Raman spectra of the hydroxyl stretching region of carrboydite, hydrohonessite, mountkeithite, reevesite and takovite

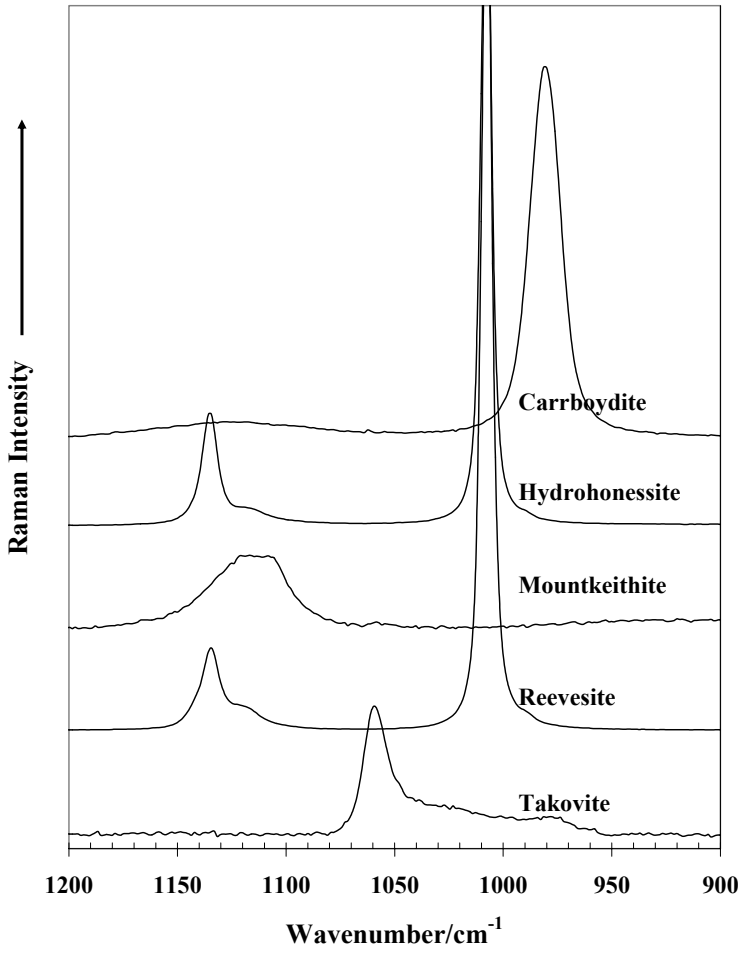

Figure 2 Raman spectra of the SO_4 and CO_3 stretching region of carrboydite, hydrohonessite, mountkeithite, reevesite and takovite

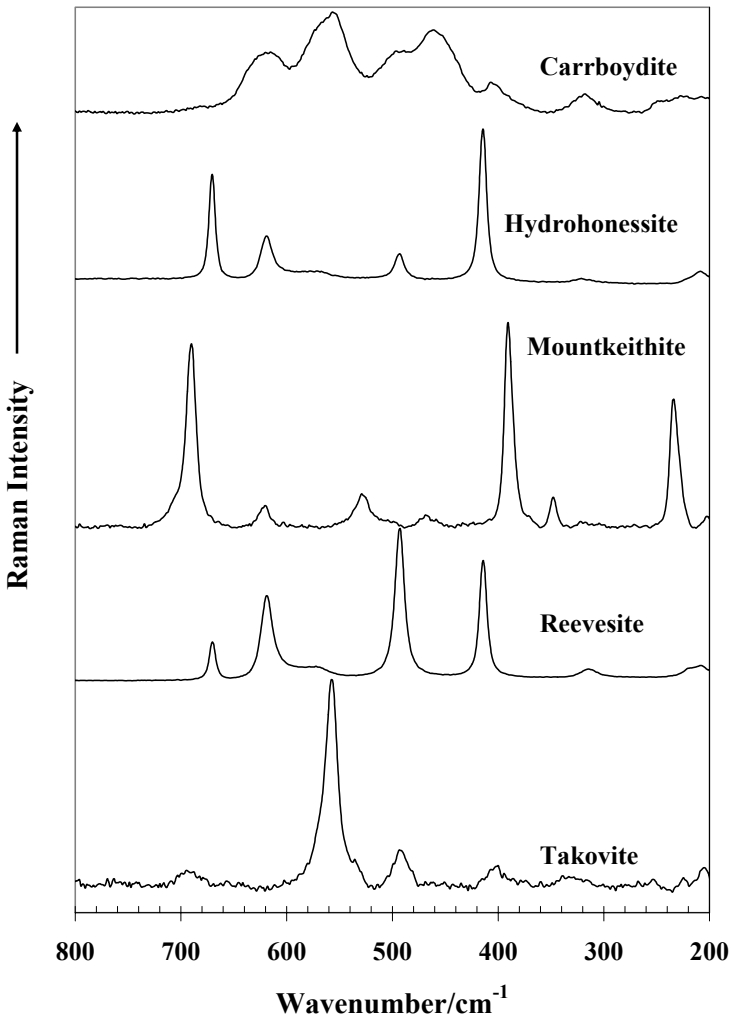

Figure 3 Raman spectra of the SO_4 and CO_3 bending region of carrboydite, hydrohonessite, mountkeithite, reevesite and takovite

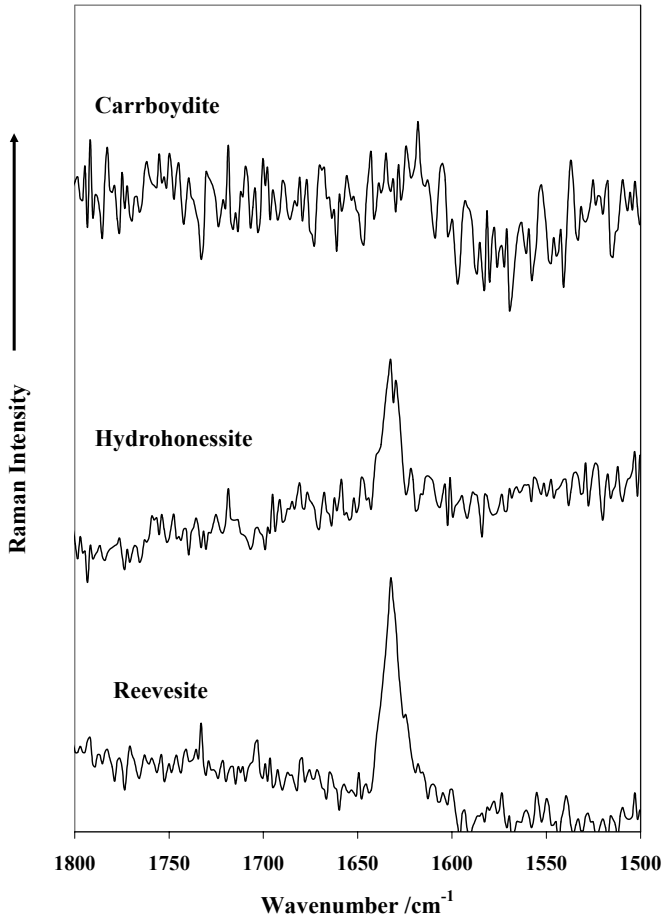

Figure 4 Raman spectra of the water HOH bending region for selected hydrotalcites